33RD CONGRESS
OF THE INTERNATIONAL COUNCIL
OF THE AERONAUTICAL SCIENCES
STOCKHOLM, SWEDEN, 4-9 SEPTEMBER, 2022

ICAS 2022 SWEDEN

DLR DESIGN CHALLENGE 2022: DESIGN OF A NEXT GENERATION VTOL FIREFIGHTING AIRCRAFT

Johannes Ritter[1], Hannes Kahlo[1], Nicolas Mandry[1], Ahmet Günay Can[1], Prishit Modi[1], Benjamin Knoblauch[1], Johannes Schneider[1], Andreas Strohmayer[1], Tobias Dietl[2], Patrick Ratei[2], Prajwal Shiva Prakasha[2] & Björn Nagel[2]

[1]University of Stuttgart, Institute of Aircraft Design (IFB), Stuttgart, Germany
[2]German Aerospace Center (DLR), Institute of System Architectures in Aeronautics, Hamburg, Germany

Abstract

Since 2017, the German Aerospace Center (DLR) has been organizing an annual student competition on conceptual aircraft design titled DLR Design Challenge. This education and training initiative is set to challenge the next generation of aircraft designers with topics tailored to current research questions in the field of aeronautics. This year's challenge was about the development of an aerial firefighting system of systems including vehicle and fleet design with a strong emphasize on operationally-driven design aspects.
This paper proposes a design for a next generation vertical take-off and landing firefighting aircraft with an expected entry into service in 2030, that is working intelligently and interconnected in a group of four. The design won the DLR Design Challenge 2022 and the underlying work covers the preliminary design including the structural concept, aerodynamic simulations, weight and balance calculations and the concept for water intake and deployment.
The designed aircraft is characterized by a considerable high payload ratio that features vertical take-off and landing capabilities while showing efficient horizontal flight properties with a very competitive cost basis. The 24-hr operability during various weather conditions and challenging fire scenarios is ensured using a wide variety of sensors and a modern glass-cockpit combining pilot comfort with indispensable safety aspects. Due to its modular design, every aircraft can be comfortably converted to a passenger or freight version during firefighting off-season or for cargo and crew supply during the missions.

Keywords: education, student challenge, aerial firefighting, aircraft design, system of systems

1. DLR Design Challenge

1.1 Motivation, Objective and History

The air transport sector is facing enormous economic and environmental challenges in the coming years. These require innovative and sustainable ideas and approaches in order to offer added value to society. In this context, since 2017, the **G**erman **A**erospace **C**enter (DLR) has held an annual competition for students to come up with futuristic aircraft concepts that are geared towards current areas of focus in aeronautics research. Herein, students can apply, test and prove their knowledge as well as skills by creatively and innovatively tackling aeronautical engineering problems. The developed designs should comprise a coherent overall concept, with a focus on the specific key theme for that year's competition. New issues are emerging in aeronautics research, particularly against the background of climate change and digitization. The design concepts should properly engage with issues that are currently critical in aircraft design, with a view to shaping the aeronautical technologies of the future with new innovations and visions. Therefore, revolutionary ideas are needed. In recent years, the DLR Design Challenge has covered a variety of topics from supersonic commercial transport over small aircraft for rural needs, hydrogen-powered aircraft and parcel-delivery drones. Fig. 1 shows the chronology of the competition including each year's theme, winning team and concept. Main goals

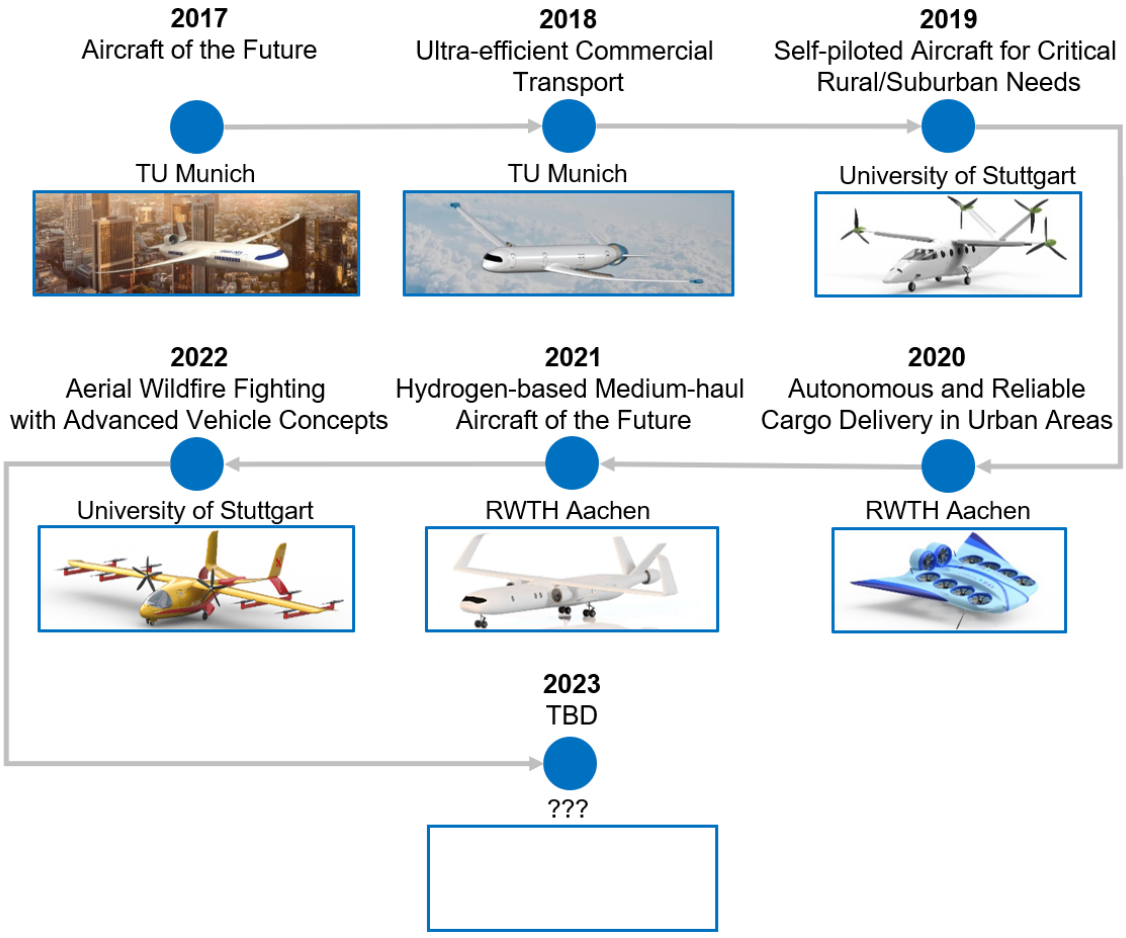

Figure 1 – Chronology of the DLR Design Challenge

have always been to design vehicles with significantly reduced environmental impact and increased connectivity of goods and people. With the COVID-19 pandemic creating some difficulties the Design Challenge became mostly digital in the last years but was never canceled. This ongoing success over the last six years will continue in the future with new topics and challenges for future aircraft designers. In the context of disaster relief and response, aerial firefighting is introduced as a new topic in 2022. For more information concerning the history of challenges and links to the underlying challenge, the reader is referred to the general DLR Design Challenge homepage [1].

1.2 Organization

Organized on a rotating basis by the Institute of System Architectures in Aeronautics and the Institute of Aerodynamics and Flow Technology, the DLR Design Challenge addresses German university students who are interested in aircraft design. A rough timeline which is followed every year can be found in fig. 2.

Teams can be registered a team with a minimum of two and maximum of six members through their university department. They receive an invitation to the kick-off event, where the task for this year is announced. Any prior work or application with a first draft is not necessary, since the kick-off event represents the first day of the competition. Therefore all participants and their university advisors meet at a DLR institute. Some general information about the Design Challenge is given, along with an introduction to the topic by experts who are dealing with the issue in their research work. After the task is officially presented, students also have the opportunity to exchange ideas with participants from other universities as part of a workshop. The aircraft designs and overall-system concepts are then be developed over a period of around four months. During this time the teams have the opportunity to ask questions in order to clarify the task description. No further technical help will be provided by DLR. The concepts have to be submitted in form of a technical report. Usually a few weeks later

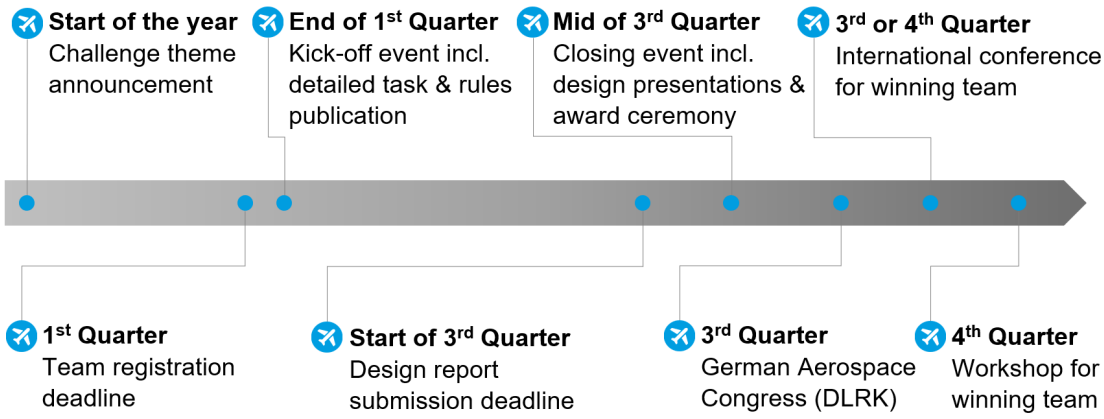

Figure 2 – General timing of the yearly DLR Design Challenge

the Design Challenge culminates in the final event, which also takes place at a DLR institute. A jury of DLR experts, consisting of several institute directors from the field of aeronautics research and led by the divisional board member for aeronautics, is responsible for reviewing and evaluating the aircraft designs. This evaluation is based on the technical reports and presentations given at the final event. Finally, the winning teams are announced and awarded. While the best three teams are given the opportunity to present their work at the **G**erman **A**erospace **C**ongress (DLRK), the winning team publishes their concept at an international aeronautics conference.

2. DLR Design Challenge 2022 on Advanced Aerial Firefighting System of Systems

2.1 Theme

Wildfires pose a tremendous threat to people, wildlife, and forestland. In the light of global warming, wildfires are an ever-increasing problem all around the world. Not only are the wildfire seasons getting longer, but the fires are also becoming more and more intense, which causes further carbon dioxide emissions. Aviation has a key position among the available firefighting assets. By reducing the fire intensity and slowing down the fire propagation, aerial suppression enhances the firefighting effectiveness and makes ground-based firefighting safer. However, the aerial suppression operations are costly and, due to aged vehicle technology, stay behind their full potential. Therefore, the ongoing development of future-oriented aeronautical systems such as unmanned aircraft systems or advanced air mobility vehicles yields the opportunity of designing modern aerial firefighting vehicles for direct suppression attacks which is also part of current research activities [2]. While there is a large design space allowing for different vehicle architectures across various weight classes, the vehicles shall enable very short or even vertical take-off and landing operations to scoop from water sources in the proximity of the wildfire area. Finally, the goal is to maximize the amount of water delivered to the fire front by the design of energy- and cost-efficient aeronautical systems.

2.2 Task

Following the theme described above, the given task does not only focus on the development of the air vehicle concept from the field of advanced air mobility but also puts a strong emphasize on fleet and operationally-driven design aspects. The conceptual designs are requested to target an entry into service in 2030 and are required to achieve certain scenario-driven mission performances. The fleet of air vehicles must be able to carry a total of 11 000 kg water in a single suppression attack, whereas the maximum take-off mass of each individual air vehicle is limited to 5760 kg. In order to continuously fight the fire, scooping from nearby water sources shall be enabled by appropriate system as well as subsystem designs. The powertrain architecture of the vehicles, the fleet size as well as the fleet operational tactics are key elements of the design space. The objective of the fleet design and operations is to maximize the amount of water carried to the fire line in 24-hours of mission time. Further information on the task can be found online. The timeline of this year's challenge is provided

in the below figure. More information concerning this year's DLR Design Challenge as well as the task is available as download can be found online [3].

2.3 Participants and Results

The field of participants consists of six teams with a total of 33 students from the following five universities: DHBW Ravensburg, RWTH Aachen University, TU Braunschweig, TU Dresden and University of Stuttgart. As a result of the relatively open request for proposals, the students' works show a wide variety of ideas and concepts as displayed in fig. 3. While the two teams Dipper & **A**erial **E**xtinguishing **G**rouped **I**ntervention **S**ystem (AEGIS) by DHBW Ravensburg and GLAROS (seagull in Greek) by TU Dresden & TU Braunschweig decide for flying boats with distributed electric propulsion, the teams Firef(l)ighter by DHBW Ravensburg and third-placed FireWasp by RWTH Aachen University chose rotorcraft configurations powered by conventional propulsion systems. Finally, the second-placed design pro**PEL**lor driven turbo **E**lectric hybrid **F**irefighting **A**uto**N**omous v**T**ol (PEL-E-FAN-T) by TU Dresden and the winning concept **IN**telligent **F**ir**E** **R**espo**N**se **O**peration (INFERNO) by the University of Stuttgart display a lift + cruise hybrid-electric VTOL configuration. Detailed information about about all submissions including reports and pitch videos can be found in the corresponding press release [4]. While all of this year's submissions were highly appreciated and valued by the jury, the team from the University of Stuttgart took first place with their design INFERNO, which is presented in greater detail in the following.

Figure 3 – Overview of all concepts as part of DLR Design Challenge 2022 (depicted in alphabetical order of university names)

3. Design of INFERNO

3.1 Wildfire Scenarios

An essential part of this year's assignment is the investigation of two forest fire scenarios in Europe. NASA's **F**ire **I**nformation for **R**esource **M**anagement **S**ystem (FIRMS) was used for the implementation and data generation as this system reports active fires within a few hours after the first satellite observation occurred. The analyzed data is from Italy and Romania collected in July 2021. These two scenarios were chosen because they have a similar magnitude and represent both a domestic and a coastal scenario [5], [6].

First, the coastal scenario was considered. The selected area includes the region of Apulia and parts of Basilicata. This corresponds to an area of about 23 000 km^2 with 201 detected fire sources. The

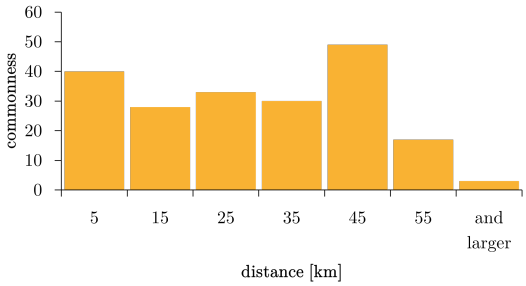

Figure 4 – coast scenario: distance sea – fire source

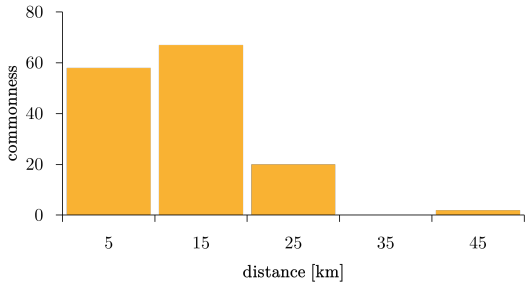

Figure 5 – coast scenario: distance lake – fire source

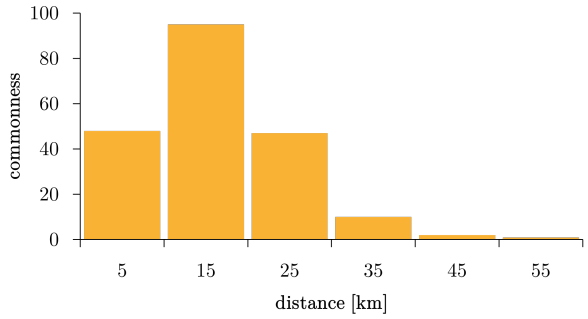

Figure 6 – Domestic scenario: distance river – fire source

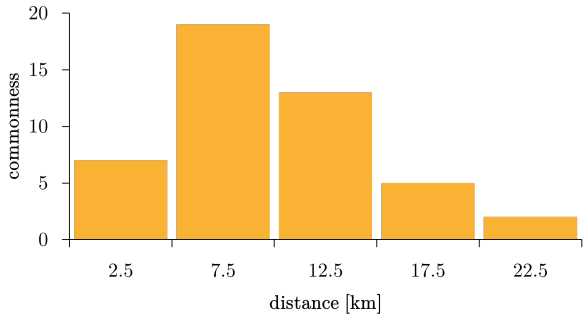

Figure 7 – Domestic scenario: distance lake – fire source

highest fire source is at an altitude of less than 500 m above sea level. In order to analyze the possible benefits of a **V**ertical **T**ake-**O**ff and **L**anding (VTOL) capability, the distance to the sea was measured from each fire source in this area. If the distance to a possible domestic water source was smaller, the distance to the lake was also measured. The minimum requirement for the lake is a width of 100 m. This limit was set due to the unknown depth of small water sources and the often considerably dried state during the fire season in summer. In 54 cases the sea was the nearest water source and in 147 cases a lake was closer to the fire. The average lake surface is 3.94 km^2. Fig. 4 shows that a considerable amount of fire sources is located between 0 and 10 km or 40 and 50 km from the sea. The average distance to the sea is 29.57 km and the maximum distance 62.5 km. Compared to the lakes, it can be seen that a distance between 0 and 20 km is particularly frequent in the coastal scenario. The average distance here is 12.65 km and the maximum distance 42.1 km (cf. fig. 5). As a second step, the domestic scenario was observed. The selected area includes the districts of Dolj and Mehedinti, which corresponds to an area of about 12 300 km^2. 210 fire sources were detected by the algorithm. The highest fire source is at an altitude of less than 360 m above sea level. Here, the same investigations as in the coastal scenario were carried out, whereby the Danube now takes on the role of the sea as it shows similar conditions for scooping. In the inland scenario, the lakes are the closest water source in only 63 cases. The average lake surface is 3.03 km^2. Fig. 6 shows that several fire sources are located between 10 and 20 km from the river. The average distance to the river is 16.89 km and the maximum distance 57.89 km. In comparison with the lakes, it becomes clear that a distance between 5 and 10 km is particularly frequent. The average distance is 11.94 km and the maximum distance 28.95 km (cf. fig. 7). It can be seen that the advantage of using small lakes is obvious in this scenario and plays a major role for both the coastal and domestic areas.

3.2 Initial Sizing – Maximizing Dumped Water

During the preliminary design phase, the optimal range for the aircraft was determined by maximizing the amount of water that is being transported to the fire during a 24 h mission. The total amount of water for one mission is set by the task to 11 000 kg. The amount of transported water during a given

period scaled linear with the flight speed of the aircraft. Because INFERNO has many acceleration and deceleration maneuvers during its mission, the cruise speed was set relatively low to 300 km h^{-1}. This is similar to other fire fighting aircraft like the CL-415 (333 km h^{-1}) [7] or the AT-802 (356 km h^{-1}) [8]. For the design mission, the distance between the base and the fire (75 NM) and the water body and the fire (15 NM) was given. In this preliminary design phase, the speed during the flight sections is considered constant and the time for approach, water refilling and take-off at the water body is estimated with 1 min. The turnaround time at the base was set to 5 min. With all these estimates, the water that is delivered to the fire within 24 h depending on the range of the aircraft can be calculated. In fig. 8, the amount of water that can be dropped by the fleet of aircraft within 24 h is displayed depending on the range of the aircraft. With an increasing range, the amount ameliorates as expected. The gradient of the graph however significantly decreases at a range of around 1200 km. To achieve an optimal balance between range and therefore fuel volume and a high water transportation rate, the preliminary design range was chosen as 1200 km.

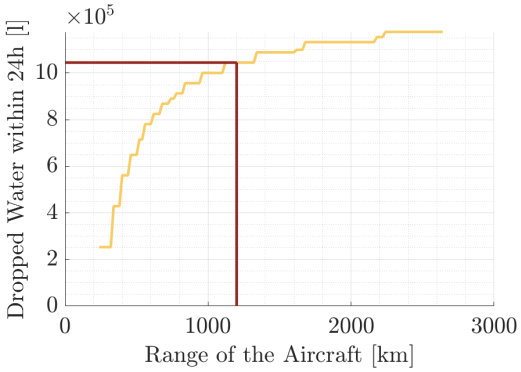

Figure 8 – Preliminary calculation of the optimal range for water maximization

3.3 Design Process

In the following chapter, the design process for the INFERNO aircraft is described. Therefore, crucial design decisions concerning the flight capabilities, the energy storage or the overall configuration are presented and justified. Due to the **M**aximum **T**ake-**O**ff **M**ass (MTOM) of less than 5670 kg and a single pilot operation, a certification under EASA CS-23 and FAR Part 23 is seeked.

3.3.1 Vertical Take-Off and Landing vs. Short Take-Off and Landing

In a first step of the design process, the advantages of a VTOL as well as a **S**hort **T**ake-**O**ff and **L**anding (STOL) were evaluated. The VTOL has the major advantage that no runway is needed for take-off. This means that smaller water surfaces can be used for water refilling. Chap. 3.1stated the clear advantage when having the possibility to use smaller water sources in the forest fire scenarios analyzed. In addition, hovering is possible and lower flight altitudes can be achieved. In favor of a configuration with STOL characteristics is the fact that the cruising speed is significantly higher and the payload share in relation to the **M**aximum **T**ake-**O**ff **W**eight (MTOW) is increased. In addition, the power requirement for the same payload is lower than for a VTOL vehicle [9]. This also means that operation and production is cheaper. To decide between these two concepts, the INFERNO team set the design requirement of combining the advantages of both concepts. This is achieved with the help of an electric drive concept, which offers significantly more degrees of freedom in the design of configurations. Due to the small space requirements of electric motors, they can be flexibly positioned or a larger number of small propellers can be used [10]. This leads to improved drive efficiency. Flexible positioning means that swivelling thrusters for vertical take-off and landing can be dispensed, resulting in a significant reduction in maintenance. In addition, a buffer storage allows the power required for short periods to be significantly higher than the available continuous power.

3.3.2 Configuration Selection and Key Technologies

To combine VTOL and STOL capabilities, a wing like that of a classic fixed-wing aircraft is indispensable. For the positioning of the wing, a high wing is almost without alternative for amphibian aircraft, as

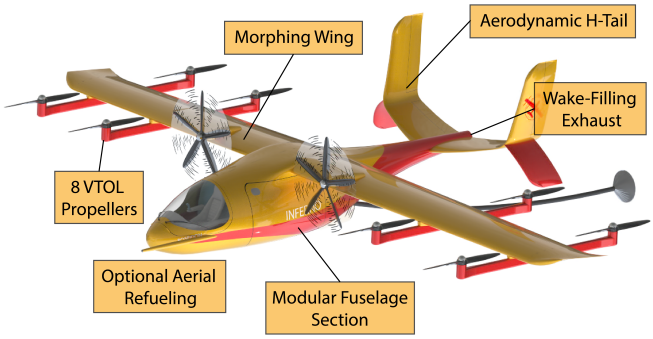

Figure 9 – Unique characteristics of INFERNO

it provides ground clearance and distance to the water during scooping [11]. There were several options for the distribution of the drives, as the electric drives offer substantive flexibility. One option was the usage of tilt rotors but the concept requires more maintenance and is more susceptible to faults and therefore results in more costs. Moreover, the **E**ntry **I**nto **S**ervice (EIS) of 2030 has to be considered during the design decisions. Thus, the INFERNO aircraft features separated propulsion systems for both vertical and horizontal flight. As shown in fig. 9, the final configuration selection is characterized by eight VTOL propellers distributed along the wing span to achieve sufficient rotor area. For the positioning of the propulsion, three options were investigated. The first option was the positioning at the rear of the tail as a pusher. Moreover, the positioning at the wingtips or classically close to the fuselage was evaluated. The pusher configuration caused ground clearance problems during take-off when the aircraft is rotating conventionally, so it was not suitable for the requirements. When comparing the other configurations, there were advantages for both. However, the advantages of the close-to-fuselage drive, and the associated support of the tail by the propeller wake, outweighed those of the wingtip propellers. When selecting the tail unit, the decision was made in favor of an H-tail unit. Since the rudder area became very large due to the short lever arm and the relatively high wing area, an H-tail has decisive benefits as it divided this area into two separated rudders, thus reducing the height. A more detailed investigation takes place in chap. 3.3.3 Fig. 9 and fig. 10 show the key characteristics, equipment and technologies of the INFERNO concept. Moreover, the aircraft dimensions are summarized in tab. 1 and fig. 12, 13 and 11.

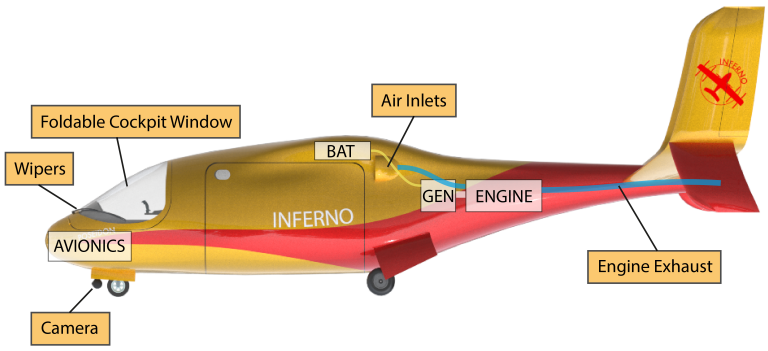

Figure 10 – Unique characteristics of INFERNO

Table 1 – Technical data of INFERNO

Aircraft Data	
Length	8.50 m
Height	3.60 m
MTOM	5670 kg
Wing Area	27.4 m^2
Aspect Ratio	9.34
Anhedral	-2°
Sweep Leading Edge	5°
Taper Ratio	0.5
Take-off Field Length	600 m
Climb Rate (hor.)	1400 ft/min
Climb Rate (VTOL)	1000 ft/min
Climb Gradient **A**ll **E**ngines **O**perative (AEO)	max. 20%
Climb Gradient **O**ne **E**ngine **I**noperative (OEI)	6%
Cruise Speed	Ma 0.25
Cruise Altitude	FL 080
Glide Ratio	16.32
Fuel Consumption Design Mission	400 kg

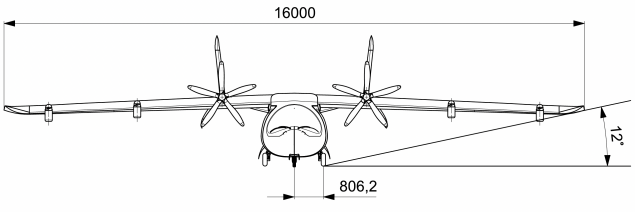

Figure 11 – Front view of INFERNO

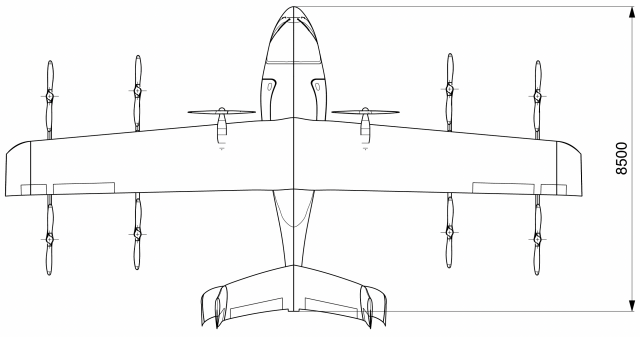

Figure 12 – Top view of INFERNO

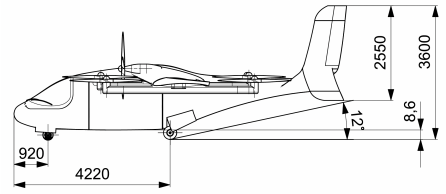

Figure 13 – Side view of INFERNO

Tab. 2 summarizes the key technologies of INFERNO. Additionally, sources are listed for the respective **T**echnology **R**eadiness-**L**evels (TRLs) that show the technical status and further development up to 2030.

Table 2 – TRL of key technologies

Key Technology	TRL
Synthetic fuels	6 [12]
Battery	5 [13]
Wake-Filling	3-4 [14]
Hybrid system	6 [15]
Morphing Wing	6 [16]
Exchangeable fuselage	4 [17]
Electric Motors	4 [18]
Sensing Instruments	6 [19][20]

3.3.3 Aerodynamics and Flight Mechanics

The aerodynamics section covers all relevant design decisions concerning the wing, the empennage and the overall aircraft.

Wing Planform Selection The general mission design is decisive for the wing planform design. The most important parameter for this is the Mach number. Due to the vertical take-off capabilities, only relatively low cruising velocities can be realized because of the expected drag from the vertical take-off propulsion system. For the targeted cruise speed of 300 km h^{-1}, the Mach number is in the range of 0.23-0.25 at 8000 ft. The mission demands good slow flight characteristics, high maneuverability and short take-off and landing capabilities when the aircraft is not started and landed vertically. The

decisions for the parameters were made using Roskam's book [11].
The wing loading was chosen in the same order of magnitude as the Canadair CL-415 [7], giving a wingspan of 16 m and a taper ratio of 0.5 with a chord length of 2 m on the wing root and 1 m on the wing tip. This results in a wing area of 27 m^2.
A lower wing loading supports the slow flight characteristics and take-off distances. The 0.5 taper ensures an equally distributed lift over the wing. This taper is achieved in 2 steps. From 2 m chord length on the wing root to 1.5 m at just over 14.5 m span and 1 m chord length on the root tip. Due to the relatively low Mach numbers, only a small sweep back of the wing is needed. Therefore a backwards wing sweep of five degrees on the leading edge was chosen so that the trailing edge is orthogonal to the fuselage. Furthermore a negative dihedral wing was chosen, which increases the maneuverability during the firefighting mission. However, the distance to the water surface when collecting water limits this angle. Thus, an angle of -2° is a compromise for these two boundary conditions. A top view of the wing is shown in fig. 12.

Morphing Wing To optimize the aerodynamics of the aircraft during its agile mission and to fulfill diverse requirements of different flight phases, the INFERNO concept is featuring a morphing wing system. The considered flight phases include rapid climb or descent to deploy or pick up water, short take-off or landing maneuvers as well as slow and high speeds phases. For conventional aircraft, the increase in lift during take-off and landing is realized through high lift devices like flaps and slats. Nevertheless, conventional lift increasing surfaces come with several disadvantages, as high lift devices increase drag by increasing camber. Additionally, noise is increased by multiple separation points on the airfoil near the trailing edge and in the separated zones between flap and wing.[21]. A morphing wing concept is diminishing these disadvantages as a smooth and continuous surface can be ensured. Moreover, the need for a high lift coefficient at low speed and a low drag coefficient at cruising speed is combined by the morphing wing technology. Nonetheless, the concept is not applied for the entire wing of the INFERNO aircraft. The wing is still featuring conventional ailerons as morphing ailerons combined with a morphing wing would increase complexity and weight significantly [22]. Thus, the outer area of the wing is using a conventional wing structure combined with conventional ailerons. Furthermore, the INFERNO has a different operational weight after water deployment. This places different demands on the wing and lift. These additional requirements are compensated by the morphing wing. The INFERNO morphing wing concept is showing differences to previously presented morphing wing designs. The system is variable in thickness over the chord depth having a variable leading edge, active camber and variable thickness, as presented by Coutu et al. [23] and Woods et al. [24], as shown in fig. 14. The combination of gas spring actuators which can modify the thickness of the **S**hape **M**emory **A**lloy (SMA) and the variable camber, realized by the **F**ish **B**one **A**ctive **C**amber (FishBAC), provide a fully variable airfoil in thickness and camber. Thereby, 80% of the tendon length is constructed as shown in Couto et al. [23] and the remaining 20% is the FishBAC. This allows differences in $\Delta C_l = 0.80$.in take-off speeds and at $\alpha = 14°$ and difference in $\Delta C_d = -0.62 \cdot 10^{-3}$ during cruise and $\alpha = 0°$. This difference in lift coefficient is almost equivalent to a plain or split flap, but without the negative effects normally associated with conventional flaps like stall at lower angles of attack or increased drag or noise.

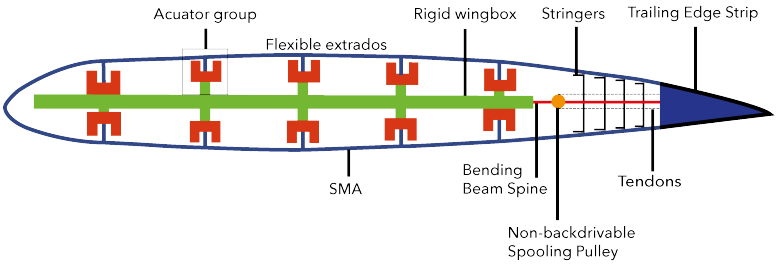

Figure 14 – Morphing wing system

Airfoil Selection In general, airfoils are selected according to the time-dominant flight phase. For civil aircraft the dimensioning phase is cruise, whereas for fighter jets this could be dogfight. The INFERNO is operating in several flight phases, as this aircraft performs 17 take-offs and landings in one operational period. Therefore, two flight phases take-off/landing and cruise were chosen for the airfoil selection. Take-off or landing require high lift coefficients, whereas the cruise airfoil must provide sufficient lift and minimize drag. The conducted research included a literature review of existing high lift airfoils and cruise airfoils for low speeds and a comparison through calculations in XFOIL. In the following paragraph, the selected airfoil of the wing and empennage selection will be described.

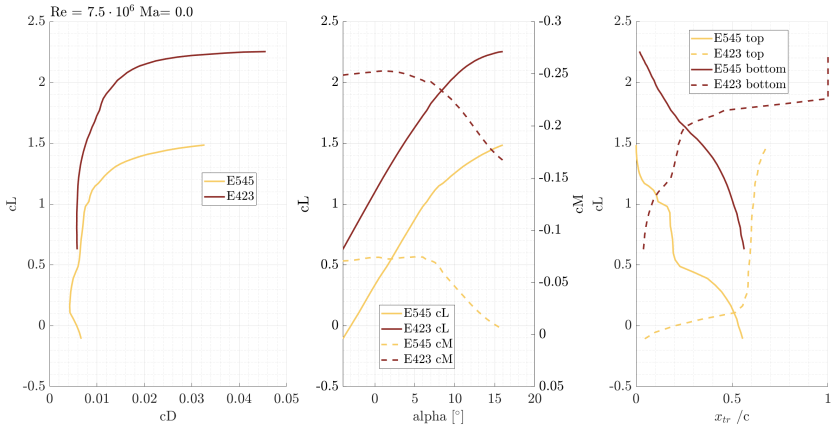

Figure 15 – Drag polar comparison of E423M and E545 airfoil for $Re = 7.5 \cdot 10^6$

Wing Airfoil Selection The large chord depth of the INFERNO and contamination from the environment disturbing possible laminar flow regions must be taken into account. Typically, for high-lift demands the E420 would be better [25] as higher lift coefficients can be obtained, but the E420 loses its high-lift characteristics under high roughness which can be caused by contamination from fire soiling or sprayed (sea-)water. As roughness and Reynolds numbers of up to Re $= 5 \cdot 10^6$ can critically affect the flight properties, the Eppler E423 airfoil was selected. The E423 airfoil is the better choice, as this airfoil can better tolerate these environments [26]. Nonetheless, high-lift airfoils are susceptible to flutter due to their thin character and are generally associated with higher structural masses. To diminish those effects, the E423 airfoil has been modified. The camber was reduced and its relative thickness was increased.The second chosen airfoil is the E545 Airfoil, which is used in general aviation applications and has an increased laminar bucket and properties which are only marginally affected by increased roughness.
XFOIL was used to analytically calculate the aerodynamic characteristics of the airfoils and to investigate the influence of Reynolds and Mach numbers which vary between Re $= 2.5\text{-}13 \cdot 10^6$ and Ma $= 0\text{-}0.25$ for take-off conditions and cruise speed. Fig. 15 show the drag polars of the E 423Modified (E 423M) and E 545 airfoil for the relevant flight phases, as the E 423M will be used for low speed conditions (Re $= 2.5\text{-}7.5 \cdot 10^6$) and the E 545 for cruise phases only (Re $= 7.5\text{-}13 \cdot 10^6$ and Ma $= 0\text{-}0.25$). Switching between airfoils is made possible by the morphing system, which is described in chap. 3.3.3

Horizontal Stabilizer Sizing The size of the horizontal stabilizer S_{HT} is calculated by eq. (1) taken from [27] with $\overline{V}_{HT}$ as the volume coefficient of the horizontal stabilizer, r_H as the distance between the aerodynamic center of the horizontal tail and the center of gravity, S_W as the wing area and l_μ as the mean aerodynamic chord.

$$\overline{V}_{VT} = \frac{S_{VT} \cdot r_V}{S_W \cdot l_\mu} \tag{1}$$

The volume coefficient for a flying boat or a general aviation, twin engine aircraft is typically around

0.7 according to [27]. All the other parameters are part of the design and are obtained via iterative calculation. According to [28] the sweep of the horizontal stabilizers ¼-chord line should be a little bit higher than the wing sweep, so that compression effects on the tail occur later than on the wing [27]. In this design 15° for the ¼-chord line and thus 17° for the leading edge is chosen. As the taper ratio 0.8 is chosen, which is a little higher than suggested by [27], but provides us with more space and structural strength for the installation of the vertical stabilizer. The calculated area for the horizontal stabilizer would therefore be 6.7 m^2. Due to the increase of the dynamic pressure at the stabilizers the size could be reduced by 43% to 3.8 m^2. The critical point for the horizontal stabilizer is the go around maneuver, where the propellers deliver 100% thrust. According to [29] the increase in dynamic pressure $\frac{q_H}{q}$ can be calculated by eq. (2) with the horizontal stabilizer area S_H, the area that is placed within the wake $S_{H,Wake}$, the power of the propellers P_{av}, the air density at the respective altitude ρ, the airspeed v and the diameter of the propellers D_P.

$$\frac{q_H}{q} = 1 + \frac{S_{H,Wake}}{S_H} \cdot \frac{2200 \cdot P_{av}}{\frac{\rho}{2} \cdot v^3 \cdot \pi \cdot D_P^2} \tag{2}$$

The dynamic pressure at the horizontal tail during go around increases therefore nine fold, that is why the reduction of horizontal tail size is permissible. In accordance with Raymer [30], the elevator size was set to 25% of the horizontal tail area and with a constant percent chord for structural reasons. Due to the vertical tail being directly connected to the horizontal tail, the horizontal tail is fixed and the trimming is done via the elevators.

Vertical Stabilizer Sizing As the horizontal stabilizer, the size of the vertical stabilizer S_{VT} is determined also by its volume coefficient $\overline{V}_{VT}$ the distance between the aerodynamic center of the vertical stabilizer and the COG r_V, the wing area S_W and the wingspan of the wing B_W and can be calculated with eq. (3) from [27].

$$\overline{V}_{VT} = \frac{S_{VT} \cdot r_V}{S_W \cdot l_\mu} \tag{3}$$

The volume coefficient is derived from literature like [30] and chosen as 0.06. The total area of the vertical stabilizer would therefore need to be 6 m^2. Due to the deft position of the propellers, the vertical stabilizers face an increased dynamic pressure as well eq. (4).

$$\frac{q_H}{q} = 1 + \frac{S_{H,Nachlauf}}{S_H} \cdot \frac{2200 \cdot P_{av}}{\frac{\rho}{2} \cdot v^3 \cdot \pi \cdot D_P^2} \tag{4}$$

The vertical stabilizers face the highest loads, when one engine fails and the increase in dynamic pressure is lowest during cruise flight. Because only one engine is operative in this scenario, only one vertical tail faces the 44 % increase in dynamic pressure. This allows, to decrease the vertical tail area by up to 22%. A vertical tail area of 4.9 m^2 is chosen, which is a 18% reduction.
The wing sweep of the leading edge is chosen as 12° (11° ¼-chord line) in accordance with [27].
40% of the airfoil chord was dedicated to the rudder surface in the upper part of the vertical tail [30], so that the lower part is free of moving parts, which makes manufacturing and maintenance easier and cheaper. The detailed sizing of both the horizontal and vertical stabilizer can be seen in fig. 12.
Since INFERNO has two vertical tails, there are no special requirements regarding spin recovery. To avoid high mach numbers and therefore high drag in the area, where the vertical and horizontal tail are joined, the position of maximum thickness of the horizontal and vertical tail does not match. Fig. 16 depicts that there are no angles that are smaller than 90° in order to keep the inference drag as low as possible.

Empennage Airfoil Selection Symmetrical airfoils are generally selected for the horizontal and vertical stabilizers [31]. NACA airfoils of the 4-series are therefore used, which have a particularly low drag coefficient. The drag coefficient in a symmetrical airfoil is only influenced by the thickness [31]. As mentioned previously, thicker profiles have less structural mass and are generally more usable to support structures. Therefore, the NACA 0010 airfoil is used for the horizontal stabilizer and the NACA 0008 airfoil for the vertical stabilizer.

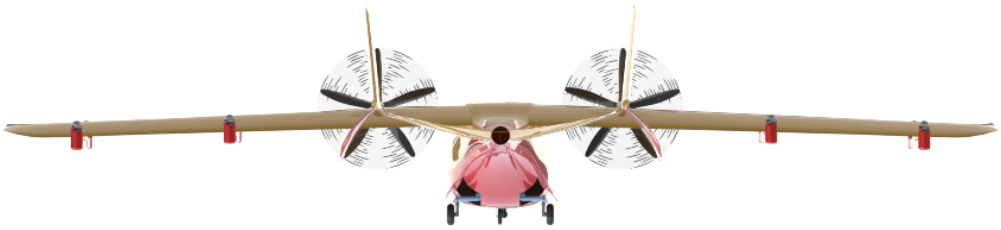

Figure 16 – Tailplane arrangement with no angles smaller than 90° for lower interference drag

Aerodynamic Calculations of the Aircraft The aerodynamic calculations of the wing were made using AERO Tool, a software tool developed by the IAG (Institute for Aerodynamic and Gas dynamic) at the University of Stuttgart. It uses the panel method to calculate lift and drag of the airfoil. Additionally, it features a XFOIL implementation to calculate the drag. The resulting lift and drag of the wing was calibrated with factors that were obtained from simulating the Airbus A320 as a reference aircraft and comparing the results with the real A320 data. Subsequently, the drag was again calibrated with textbook methods from [30], [32] and [33], to account for the drag of the fuselage. The lift of the fuselage during the flight due to its angle of attack was neglected, because its area is relatively small compared to the wing size. Because of the morphing wing concept (chap. 3.3.3), the airfoil can be changed in-flight. The cruise configuration was simulated using cruise conditions, and the high-lift configuration was simulated assuming approach or take-off conditions. Fig. 17 shows the resulting lift to drag ratio in cruise and high-lift wing configuration.

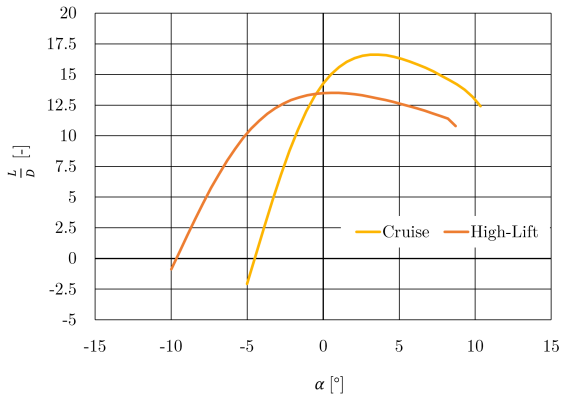

Figure 17 – Calculated Lift to Drag ratio for Cruise and High-Lift Wing Configuration

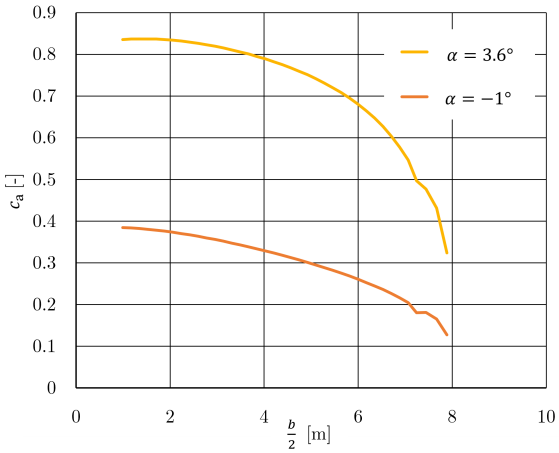

Figure 18 – Distribution of the lift coefficient for cruise flight with different angles of attack

AERO Tool does not return the stall characteristics of the wing and shows convergence problems when the angle of attack causes the flow to separate. Therefore, the graph in fig. 17 is interrupted when stall occurs. The wing planform and the resulting local lift coefficient distribution prevents an early tip stall guaranteeing controllability even when the flow starts to separate in the center of the wing. When the aircraft is about to drop the water, pilot sight is very important, so that the water can be placed as effective as possible, this is achieved by a low angle of attack for cruise flight with payload. At MTOW the angle of attack is about 3.6° and at OME at about -1° in cruise configuration. This big difference is due to the relatively high payload ratio. Nevertheless, the maximum aerodynamic efficiency stays within this range.
The morphing wing system replaces high-lift devices. The maximum lift coefficient however is not sufficient to do a horizontal take-off with MTOW, this is why the vertical propellers are supporting the take-off and climb at low speeds with high take-off mass.

3.3.4 The Hybrid Configuration

Due to the VTOL capability, surges in the power demand occur, which only last for a short amount of time (less than one minute). Furthermore, INFERNO has more propellers than on a conventional airplane (eight motors for vertical take-off and two for horizontal flight). Both of these factors are ideal for installing a hybrid energy system.
Fig. 19 shows a schematic overview of the energy system being installed in the aircraft. The eight propellers for vertical flight are powered by 250 kW electric motors, and the two propellers for horizontal flight use a 600 kW electric motor each. In the middle of the wing, the 60 kW h battery pack is placed. Behind the payload module, the generator and the power electronics are installed. The generator is directly powered by the turbine engine. A conventional turbogenerator (**G**eneral **E**lectric (GE) H85-100) powered with kerosene or **S**ustainable **A**viation **F**uel (SAF) is used, to keep the required ground support equipment and technological risk at a minimum. Due to the redundant energy system from the relatively high capacity battery and the turbine engine, no **A**uxiliary **P**ower **U**nit (APU) was installed. More detailed information on the powerplant sizing and selection of the individual components will be published at the DLRK in 2022 [34].

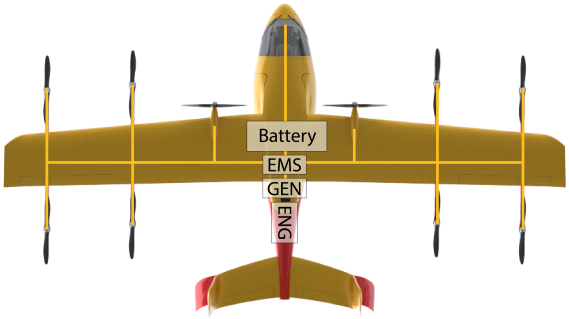

Figure 19 – Illustration of the hybrid energy storage system

Engine Air Intake and Exhaust The engine is supplied with air from both sides via air intakes see fig. 9. They are positioned high enough to prevent splash water from getting in. Unlike other aircraft, the exhaust gases are not discharged directly behind the engine out of the air frame, but are routed to the rear through the tail boom, where they flow out. The air flow is also shown in fig. 10. The exhaust gas flow is used to reduce the drag of the fuselage via wake filling, which is currently the subject of research. The CENTRELINE project [35] is investigating the possibility of increasing efficiency by introducing additional energy centrally at the tail. One of the findings is, that not too much thrust in relation to the total thrust is required to reduce fuselage drag significantly [36]. Even though INFERNO only uses the exhaust gas with its residual energy for Wake Filling, a noticeable drag reduction should be achieved. For detailed predictions, extensive **C**omputational **F**luid-**D**ynamics (CFD) simulations are required. The exhaust pipe is made out of heat resistant materials, like nickel-chromium alloys [37]. Because the exhaust gas is discharged in the rear, the tailboom faces no hot exhaust temperature from the outside, like it would, if the exhaust gas is blown out closer to the engine. The CENTRELINE project is scheduled to have a EIS until 2035. However, INFERNO's wake filling is not of this magnitude and does not use an extra propulsion unit at the rear but only uses the remaining energy of the exhaust gas. Therefore technical maturity should be given until 2030.

3.3.5 Mass Calculation and Balance

The calculation of the mass of the individual components is the basis for the calculation of the **O**perating **M**ass-**E**mpty (OME) and the **C**enter **o**f **G**ravity (CoG). There are different methods for determining the mass of the individual components. In this report, the method by Nicolai as described in Gudmundssons book [38] is used. This method is based on a series of statistical equations. In order to optimize the results, calibration was performed with two reference aircraft (Cessna 404 and AK 4). For this purpose, the masses of the reference aircraft were first calculated using the same formulas followed by the determination of calibration factors using the known masses. However, those

factors produced implausible results because both aircraft are heavily different in size compared to INFERNO. The component masses of a similar aircraft were not known. Thus, a plausible calibration was not possible. The results of the calculation can be found in tab. 3. Nikolai only calculates the mass for the entire landing gear, for the CoG calculation however, it is important to have separate masses for the nose and main landing gear. The share of the nose landing gear on total landing gear mass was estimated to be 1/3 and the share of the main landing gear 2/3 respectively.
The mass of the engine, generator (including Power Electronics), electric motors and the battery were estimated more thoroughly in the paper for the DLRK 2022 [34].In order to determine the aircraft's CoG, the position of the individual components is required in addition to the individual masses of the components. A detailed design must be available for this purpose (cf. fig. 13). The static margin is in the range of 5.7% to 25.4% of the reference wing length (see. Fig. 20). The maximum shift of the COG during a load case is less than 18 percentage points of the reference wing length. Fig. 20 and 21 show the required diagrams of the static margin and the absolute position of the CoG in respect to the MAC for **S**tandard **M**ission-**P**ayload (SMP). Respective calculations were also done for **M**aximum **P**ay**l**oad (MPL) and the ferry range loading. As shown, the required static margin and stability can be maintained during the entire mission.

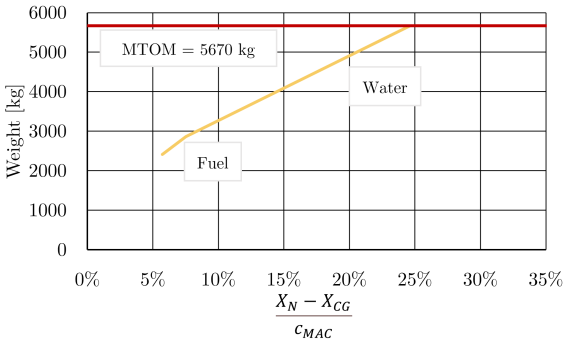

Figure 20 – Static Margin during water and fuel loading with respect to the MAC in the Design Mission

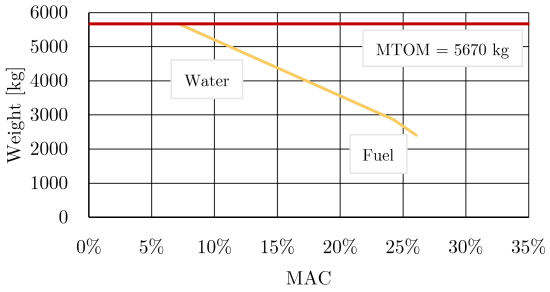

Figure 21 – Shift of the CoG during water and fuel loading with respect to the MAC in the Design Mission

Table 3 – Mass of the aircraft, fuel and water and its lever arms measured from the nose for the calculation of the COG

	Mass [kg]	Lever Arm / COG [m]
Manufacturer Mass-Empty (MME)	**2310**	**3.7** (24%MAC)
OME	**2410**	**3.8** (26%MAC)
Fuel	460	3.6
Water / Flame Retardant	2800	3.2
MTOM	**5660**	**3.5** (7%MAC)
Maximum Zero Fuel Mass (MZFM)	**5410**	**3.7** (20%MAC)

3.3.6 Cockpit

An ergonomic and operation centered approach is adopted for the development of the preliminary concept for INFERNO's single pilot glass cockpit. The glass cockpit has the dimensions 1169 mm × 1663 mm × 1436 mm (H × L × W) and has optimized pilot workspace with state-of-the-art instrumentation. The flight deck is 592 mm high and 989 mm wide with six electronic display screens for a reliable flight operation and improved pilot performance. Figure 22 outlines the dedicated cockpit displays.
Pilot performance based on psychology, physiology, and awareness depends highly on the human factors engineering [39]. To validate pilot commands, the cockpit uses intuitive control features including verbal and mechanical outputs. The cockpit also enables better guidance and control,

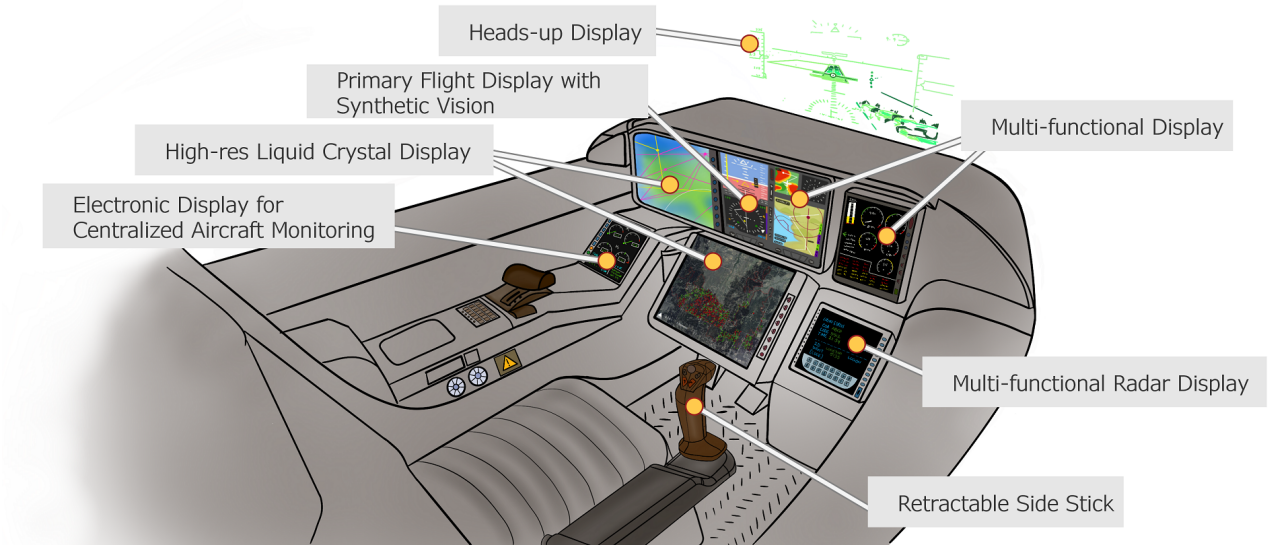

Figure 22 – INFERNO cockpit design concept with integrated instruments

thanks to several additional features, including an alerting system for emergency indication, LCDs to maintain a "static dark" environment, and larger touchscreens for effective human-machine interaction. The larger synthetic vision touchscreens provide increased readability, wider **F**ield of **V**iew (FOV), consistent luminance, increased situation awareness and uninterrupted operation during instrument flight conditions [40]. In turbulent conditions navigating through display functionalities via touch is made redundant through integrated display controller consoles (buttons). The adjustable cockpit seat accommodates a range of pilot dimensions, and its positioning also enables a primary horizontal and vertical FOV of the flight deck very well within the requirements defined in [40].
A continuous 24-hour operation capability of the INFERNO aircraft is achieved by improved ease of accessibility of the pilot to the primary control instruments, display panels and hand consoles. The pilot governs the sidestick with the right hand and controls the throttle with the left. A preliminary 2-D design of the INFERNO cockpit is illustrarted in fig. 22.

3.3.7 Sensing Instruments

A task as complex as aerial surveillance and wildfire suppression necessitates handling multiple concurrent circumstances in mid-air. A pilot relies on visual assistance and real-time reports from the ground crew during flight operations and it is essential that the pilot in the INFERNO glass cockpit accurately perceives the surroundings and is fully informed of the ground scenarios. Modern sensing equipment integrated into the INFERNO cockpit shall allow the pilot to operate effectively for a continuous 24 h day and night mission duration in terms of firefighting and effective delivery of humanitarian aid.
The pilot visualises the ground scenarios in colour and infrared with the help of an **E**arth **O**bservation / **I**nfrared (EO/IR) surveillance system. It also helps the pilot see through dense smoke in low proximity fly-by events. The weather surveillance radar provides real-time monitoring of environmental meteorological factors, and a multi-functional hybrid aircraft tracking and communication device enables uninterrupted aircraft to ground communication. For a 3-D mapping of the terrain below, an airborne laser scanner could also be integrated into the aircraft's belly with a minor dedicated design change. A list of embedded sensing instruments and their detailed functionalities is presented in tab. 4 below.

Table 4 – Sensing instruments with dedicated functions enabling 24 h operation capability (* indicates optional but feasible technology)

Instrument	Function
EO/IR surveillance system	Gyro stabilized thermal & daylight camera, laser rangefinder, onboard low-light & image blending, real-time heat map & temperature profiling, GPS [41], [42]
Weather surveillance radar	Real-time meteorological data, detection of hazards and debris
Satellite and cellular hybrid aircraft tracking and communication device	Flight data recording & monitoring, data offload, internet access, satellite & cellular voice calls, continuous satellite & cellular tracking [20]
Airborne laser scanners *	Quick & precise high altitude 3D-Scan, ground vegetation mapping, forest height & density recognition [19]

3.3.8 Water Pick-Up and Dropping

As wildfires spread rapidly in time and space, it is critical for any aerial firefighter to pick up water in the shortest time possible. In addition, certain water collection methods are restricted in space as these require particularly large amounts of space, such as scooping. In the following chapter, two water collection methods are presented that are installed in the INFERNO, scooping and intake via immersion. Afterwards, the water-release system is described.

Scooping Scooping is a well known and proven method which is already used in the firefighting aircraft, such as the CL-415. In scooping, a water source is overflown and an inlet is submerged, as the forward movement in flight collects water by means of dynamic pressure. The INFERNO has two inlets, which allow lower momentum forces and quicker refilling of the water tank as the refilling of the water tank with a single inlet would be retarded due to baffle plates in the tank. With scooping, in contrast to immersion, the entire tank can be filled. The aircraft will scoop with a speed of v_{Flight}=30 m s^{-1} and a total inlet area of $A_{\text{Inlet,S}} = 0.015\,\text{m}^2$. The tank capacity is $V_{\text{Tank}} = 3\,\text{m}^3$ and the outlet to the tank is at a height of $h = 3\,\text{m}$.

$$v_{\text{Inlet,Tank}} = \sqrt{v_{\text{Flight}}^2 - 2gh} \tag{5}$$

This results in the flow rate and the time to fill the tank.

$$\dot{V} = v_{\text{Flight}} \cdot A_{\text{Inlet,S}} \tag{6}$$

$$t = \frac{V_{\text{Tank}}}{\dot{V}} \tag{7}$$

Based on these formulas, the distance to fill the tank is calculated to be 207 m and the tank is filled in a time of t=7 s.

Immersion The process of immersion is generally used by helicopters carrying large water buckets. These buckets create a large amount of drag and can be dangerous, as helicopter pilots have to estimate the distance between buckets and ground objects and avoid entangling with static ground objects. Therefore, utilizing the fuselage as a bucket negates both disadvantages. Additionally, immersion takes a fraction of time of conventional water pick-up methods and small bodies of waters or medium-heavy seas can be approached. The immersion process starts by approaching any body of water and slowly descending near surface level. Then two flaps on the underside of the fuselage are opened, and the horizontal propellers completely halt, only the vertical propellers are operating. Slowly, the fuselage is submerged to a depth of $h_{\text{I,Depth}}$=0.8 m. After reaching the desired depth, the flaps on the underside of the fuselage are closed together with the venting and refilling valves in the upper tank area. The vertical propellers start running at full power until an altitude appropriate for the pilot is reached. Meanwhile, the horizontal propellers start until a safe speed is reached for the VTOL propellers to be shut off.

The inlet area for the immersion process is set at $A_{\text{Inlet,I}}$=0.4 m^2 and the tank is filled to a volume of 2 m^3. As the aircraft descends with a velocity of 1.11 m s^{-1}, to prevent any unsettling of the pilot or aircraft, the depth of immersion of 0.8 m is reached in 1.4 s. The average area of the tank is A_{Tank}=2.78 m^2 and the time to fill the tank is derived from the following eq. (8):

$$t = \frac{A_{\text{Tank}}}{A_{\text{Inlet,I}}} \sqrt{2 \frac{h_{\text{I,Depth}}}{g}} \tag{8}$$

Therefore, the water fill-up during immersion takes 3 s.

Water-Release System Forest fires can behave differently depending on fuel type, humidity, wind strength and slope [43]. For light forest fires it is enough to moisten the fuel with 2 L m^{-2} to suppress fire for 20 min and for bigger fires 5 L m^{-2} are enough. However, some sources assume 0.10 L s^{-1} m^{-2} to extinguish severe forest fires [44][45]. Therefore, a one-size-fits-all solution is impractical because either water would be wasted, or not enough water would be used. This calls for a variable water-release system which can deploy enough water.
The flow rate $\dot{V}$ is depending on multiple variables such as the in tank water height h_{w}, which influences maximum outflow speed $v_{\text{o,max}}$, and outlet area A_{Outlet}. As the outflow takes place without additional pressurization, the Toricelli eq. (9) can be used, which calculates the time of the entire outflow process. The time to empty the tank is described by t_{o}. This allows the average outflow speed to be determined which influences the mass flow rate. Then, the amount of water reaching the fire $\dot{A_{\text{e}}}$ can be calculated, as shown in eq. (12). A conservative loss factor of 0.7, due to misting, is suggested [43].

$$t_{\text{o}} = \frac{A_{\text{Tank}}}{A_{\text{outlet}}} \sqrt{\frac{2h_{\text{w}}}{g}} \tag{9}$$

$$v_{\text{o,max}} = \sqrt{2gh_{\text{w}}} \tag{10}$$

$$\bar{v_{\text{o}}} = \frac{1}{t_{\text{o}}} \int_0^{t_{\text{o}}} v_{\text{o,max}} dt \tag{11}$$

$$\dot{A_{\text{e}}} = \frac{A_{\text{outlet}} \cdot \bar{v_{\text{o}}} \cdot \rho_{\text{water}} \cdot 0.7}{v_{\text{Flight}}} \tag{12}$$

Based on the previously shown equations (cf. eq. (9) to eq. (12)) and considering the required volumes of water, an outflow area of 0.05 to 0.15 m^2 must be used to provide the necessary flow rates.

3.3.9 Structure and Loads

In the following section, the structural concept of the INFERNO and its modules is presented. Moreover, the chapter describes the concept of the water tank and the allocated refilling and dumping mechanisms on a structural level.

Structural Concept of the Aircraft The structural concept of the INFERNO aircraft is characterized by the ability to withstand high loads during firefighting and scooping maneuvers while also considering a lightweight construction for a minimum **O**perating **E**mpty **W**eight (OEW). The primary structure consists of stringers and frames with two reinforced frames for the connection with the modular section. The density of stringers is higher in the upper and lower part of the fuselage as these parts of the aircraft encounter higher forces e.g. through the wing mounting or the landing gear integration. As shown in fig. 28, the complete structural integrity is only possible with the module installed. Fig. 23 depicts the fuselage wing structural concept of the wing. The wing structure consists of spars and ribs as well as pylons for the VTOL propeller integration. The front spear should be positioned at between 15 % and 30 % of the wing depth while the rear spear should be located at 67 % to 72 % in accordance with the positioning of the ailerons, the morphing wing actuators and the battery integration in the

central wing box [33]. For additional stability, ribs were used for each wing in a span-wise direction. As the fuel tank is located inside the wing, the ribs have to guarantee the fuel flown inside the integral tank. The battery integration concept is shown in fig. 24. The tail section is featuring a higher density of frames in order to realize enough stability for the mounting of the vertical tail and for the rudder forces which have to be transferred to the fuselage.

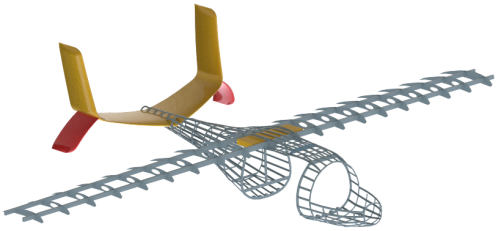

Figure 23 – Structural concept of wing

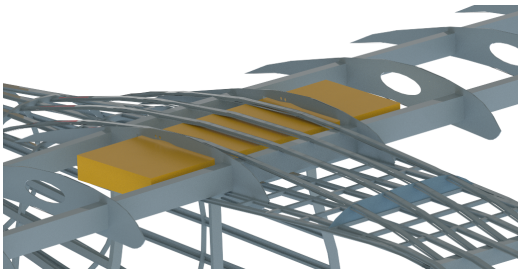

Figure 24 – Structural concept of wing and battery integration

Structural concept of the modules The modular part takes up a large part of the fuselage and cross-section, thus its capability to transfer loads during flight is essential for a safe operation. A structure of stringers and frames ensures compliance with the load transfer requirements. In the front and aft section of the module where the connection to the fuselage is made during assembly, the frames are reinforced and also feature specifically designed areas for the bolting connections. In the lower area of the module, the stringers are also reinforced as this section has to withstand high bending moments and longitudinal forces.

v-n Diagram The v-n-diagram describes the aircraft limit load factors as a function of the flight speed. The limit load factors are defined as multiple of the standard gravity constant. Usually the highest loads that occur on an aircraft are generated by the lift during high-gravity maneuvers [30]. For lower flight speeds, the maximum load factor is limited by the maximum lift available, while at higher flight speeds it is limited by an arbitrary value that was chosen in the design of the aircraft [30]. Fig. 26 shows the calculated v-n diagram.

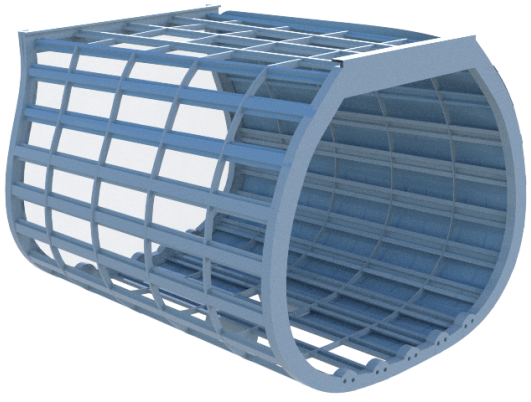

Figure 25 – Structural concept of the modules

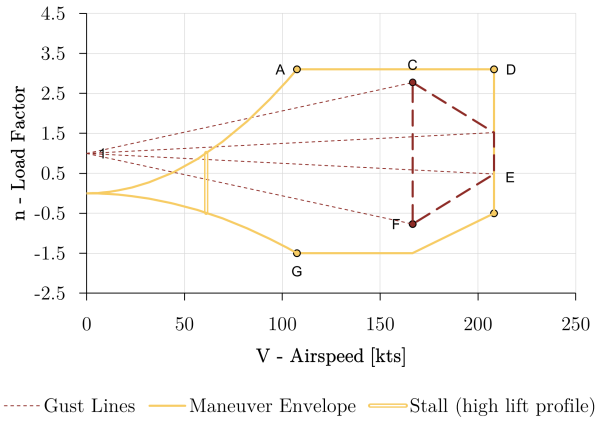

Figure 26 – v-n diagram

Concept of Water Tank The water tank is designed as an integral tank within the modular concept of the INFERNO in order to maximize the amount of water that can be carried with the module. As shown in fig. 27 which depicts the sectional view of the symmetrical tank, which is divided into three

main sections with two separations in between. Thus, swapping water during maneuvering can be prevented. Moreover, the concept features two openings in the upper forward section for water filling on ground and to balance the pressure during refilling. As described in chap. 3.3.8, the INFERNO aircraft provides two mechanisms for refilling water during the mission. The scooping maneuver is using the two scooping inlets, water dropping and water refilling during hoovering is fulfilled by the water bay doors. The two water bay doors each feature two independently operable valves, which enables precise dropping maneuvers for different missions.

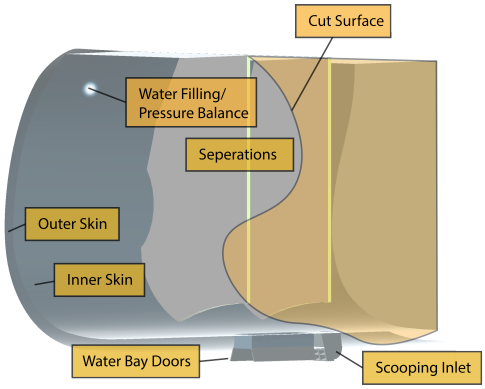

Figure 27 – Concept of water tank

Figure 28 – Structural concept of fuselage with module installed

3.3.10 Minimising Hazards and Failures

During the design of INFERNO, diminished hazards and failures that endanger the safe operation of the aircraft was a key priority. Operating safely even in exceptional situations is essential for an effective firefighting operation. Both the vertical and horizontal electric motors are redundant so that controllability is still ensured in the event of a failure. In case of an engine failure, a restart or emergency landing can be initiated by the energy contained in the buffer battery. In the event of battery failure, it is possible to continue flying with reduced power provided by the turbine on a permanent basis. Due to the configuration similar to a fixed-wing aircraft, an emergency glider landing can still be initiated in the event of a complete failure of the propulsion unit. Due to this redundancy concept, no APU is necessary. As the water can be dropped in case of an emergency, critical flight phases with high payload can be avoided in an emergency. During the design process, a strong focus was put on the reduction of mechanically moving parts. By keeping moving equipment to a minimum (e.g. fixed pitch instead of variable pitch propellers) and the elimination of a flap system, manufacturing and maintenance costs and the probability of failure can be reduced. Moreover, the advanced cockpit systems ameliorates the safety standard of the INFERNO by assisting the pilot in various weather conditions and mission phases.

3.3.11 Configuration Summary

Fig. 29 depicts the payload-range diagram. The fuel ratios for engine start and warm-up, taxi, take-off, climb and landing were taken from Roskam [11] but were reduced due to the lower cruise altitude and operation at small airports, that usually don't require a long taxi period. For CS-23 aircraft, there are no general regulations for additional safety fuel [46]. However, to operate the aircraft as safely as possible, extra fuel for an additional climb and for a 70 km flight to alternate airport, descent and landing were added. The value of 70 km was chosen, as according to [47], for 95% of airports in Europe and 99% of airports in the United States of America an alternate airport for INFERNO can be found within 70 km. For missions where alternative airports are located further away, more safety fuel should be reserved. However, due to the VTOL capabilities, the aircraft can be landed safely even at provisional bases.

The maximum payload is 3000 kg and the range with this payload is 560 km. The standard mission payload is 2800 kg per aircraft, which leads to a design range of 1200 km, as calculated in chap. 3.2

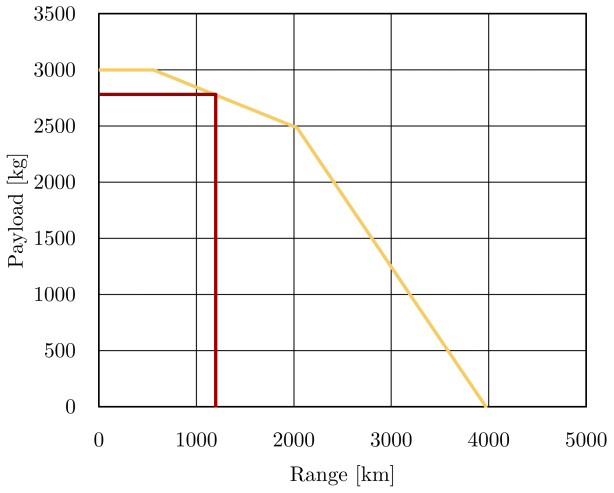

Figure 29 – Payload-Range diagram

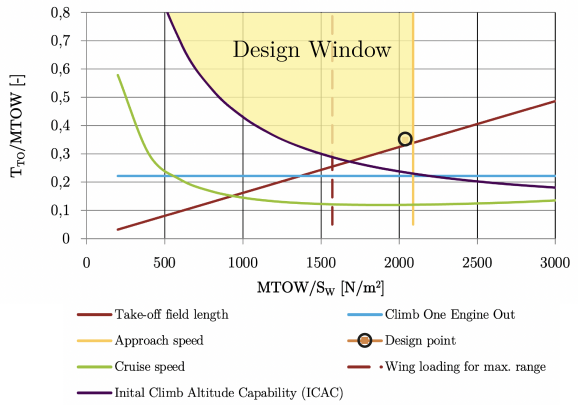

Figure 30 – Sizing diagram

The ferry range is 4000 km, which enables INFERNO to flexible proceed within Europe and Northern Africa without limitations.

3.4 Fleet Concept

In the following chapter, the unique fleet concept of the INFERNO aircraft is described, including the flexible modular design as well as its operational concept.

3.4.1 Modularity

Due to its modular structure, INFERNO is able to fulfill a wide range of tasks. Customers will be able to choose between three modules when it goes into service in 2030. More modules could be offered at a later date. In addition to the firefighting module, there will also be a cargo version and a passenger version. The cargo version with a maximum load of 3000 kg has two swiveling side doors, which ensures easy loading, even with large items (cf. fig. 31). The cargo can be secured through eyelets of the flat cargo floor. The passenger version has 5 seats arranged opposite each other (cf. fig. 32). The cross-section is designed so that all seats have a minimum seat height of 0.95 m. Behind the second row of seats, there is space for smaller pieces of luggage. Boarding and de-boarding is done via a door on the left side of the module. It opens in a way ensuring that passengers are protected by the door from the propeller. This is especially important in case of emergency evacuation.
In the following, a few explanations about the installation of the exchange module will be given. To avoid unnecessary stress on the structure in the upper section during the assembly process, no payload should be on board for the replacement and the fuel should be drained. The replacement process is carried out in four steps. In the first step, the left propeller is folded up. To reduce the maintenance effort and complexity, the folding mechanism is only possible in the ground position. Subsequently, a tail support must be attached, since the COG position cannot be covered by the landing gear without the module. Now the desired module can be transported to the aircraft with the help of special forks. The special forks are forks that are adapted to the shape of the module. The module is then transported as close to the ground as possible to the aircraft and positioned in the X direction. In the third step, the module is then retracted into the fuselage in the Y direction and raised in the Z direction. In this position, the module can be inserted into the guide rollers provided. To be able to retract the module quickly and without damage, the right outer shell is smaller than the left one. The guide rollers are conical, which means that the module is automatically centered in the X and Z directions when it is retracted. When the module is fully retracted, it is bolted to the stringer flange. In this way, the module can also transmit forces in the longitudinal direction. The bolting mechanism is designed with the help of a cardan shaft so that it can be fixed from the outside. The tail support can then be removed again. Finally, the propeller can be folded down again. The module is disassembled in reverse order.

The modular approach not only offers the operator a very high degree of flexibility, but can also ensure high utilization of the aircraft throughout the year thanks to the rapid replacement process (cf. chap. 3.4.2). Furthermore, all versions can be produced on one production line. Only the production of the modules has to be differentiated. This means that modularity is also characterized by low costs (cf. chap. 3.5).

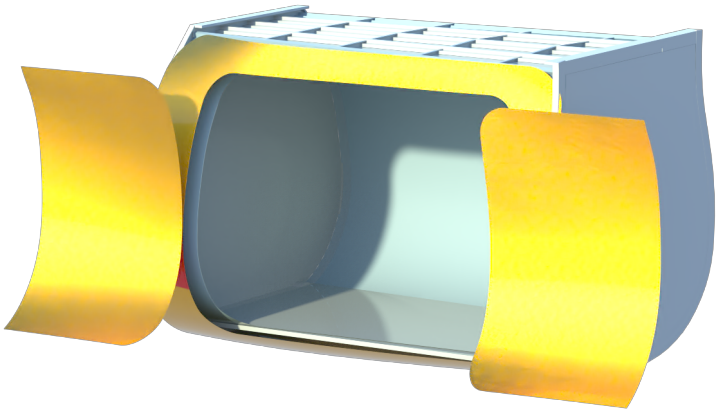

Figure 31 – Cargo version

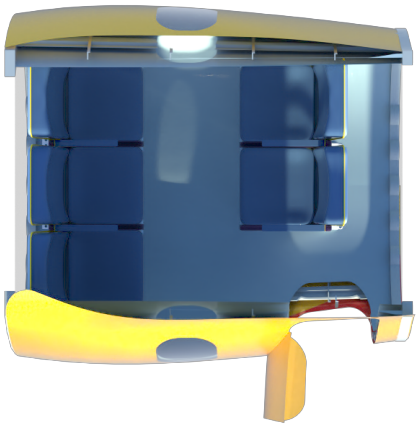

Figure 32 – Passenger version

3.4.2 Operational Concept

This section provides an overview of the operational concept on a daily and yearly basis and presents further operational aspects that characterize the INFERNO aircraft.

Operational Concept 24-Hour Mission The operational concept of the INFERNO firefighting mission is designed to optimize the amount of deployed water during a 24 h mission. For the intended mission, four firefighting aircraft are needed in order to achieve the necessary amount of dropped water within one approach of the fleet. For a successful 24 h operation, a total of 10 flight crews are necessary in order to guarantee enough rest times and work hour limits for the crews. At the beginning of each mission, the INFERNO aircraft are ferried to the operational base for the intended firefighting mission. They are accompanied by one INFERNO aircraft equipped with the passenger module and one with the freight module. The PAX version is carrying five additional pilots for the mission, while the cargo version is carrying necessary equipment like water pumps, material for a field base for the mission planning and crew preparation, spare parts and tools. Furthermore, the PAX version has to carry one additional pilot, who is positioned on a jump seat within the module. After reaching the operational base for the mission, the four firefighting aircraft named Poseidon, Taru, Fons and Aegir are prepared for the operation with the water tank being filled, the aircraft being refueled and the pilots preparing the aircraft for take-off. The additional PAX and freight version are ferried to the next mission or can be used for aerial refilling and observation or as back-up aircraft in the case of technical issues. For the first mission, four crews which could rest during the ferry flight with the PAX version are planned to be in control. As the INFERNO concept features an optional aerial refueling capability, the two scenarios have to be considered separately. Figure 33 shows the operational concept, including the refueling in flight. As shown, the flight time of several flights can be doubled and returns to the base can be minimized. By using this concept, six proceedings to and from the operational base can be avoided, which equals an additional flight time within the mission area of 6 h. Nevertheless, the aerial refueling feature is not suitable for every mission and the INFERNO fleet can also be operated without this feature.

Annual Operational Concept A yearly operation plan for the INFERNO mission is dependent on the wildfire seasons, which may be examined by looking at the number of wildfires that occur each year and the corresponding quantity of burned land around the world. The region of operational relevance for the preliminary concept design addressed in this section was decided to be Europe.

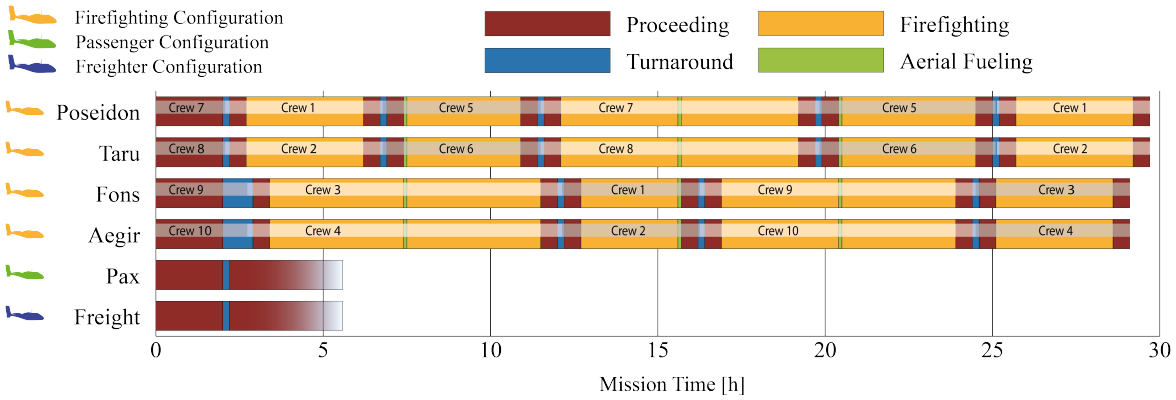

Figure 33 – Fleet concept of the INFERNO aircraft using the aerial refueling capability

Wildfire trends and cumulative burned area per month across the span of past 15 years (2006 to 2021) is publicly available on the European Forest Fire Information System (EFFIS) of the EU Copernicus program [48], [49]. The yearly low, moderate, and peak wildfire seasons across the continent of Europe and the total surface area impacted on a monthly and daily basis were then determined by statistically analysing the data retrieved from EFFIS. The EFFIS essentially provides statistics for the cumulative area burned from the wildfires after they have been successfully extinguished. Wildfires spread extremely quick in grasslands and forests, and it could take hours or even days before one is recognized by the authorities. For INFERNO's annual operational concept, due to the extreme uncertainty of when the exponentially growing wildfire would be recognized, it was assumed that 70% of the total burned area is already destroyed, before authorities recognize the wildfire and respond to it. To prevent further wildfire propagation, the course of action would be to spray down the extinguishing agent across a 20 m circumference width around the wildfire. With further intermediate calculations, the average surface area to be extinguished per day was calculated to approximate the average number of INFERNOs required per day per month of the year to fight European wildfire. An additional INFERNO is also assigned to the firefighting batch with rescue and cargo capability in the form of extended humanitarian aid for the distressed victims of the wildfire.

The annual operating concept for Europe (**E**uropean **U**nion (EU) + Non-EU) calls for a maximum of eight INFERNOs, i.e., a fleet of 32 aircraft with eight of each Aegir, Fons, Poseidon, and Taru aircraft, are deployed for a 12-month firefighting campaign across the continent. Since not all months experience equally intense wildfires, several Poseidon, Fons, and Taru are given fleet duty as cargo and passenger (Pax) aircraft, respectively, during the season of relatively less strenuous wildfires. Aegir is sustained for a yearlong firefighting duty and is accompanied continuously in operation with its other fleet members depending on the mission definition and wildfire severity. A vivid graphical representation of the yearly operation concept comprising the annual fleet management concept is realized in Fig. 34. The cumulative annual operation time of INFERNO operating in Europe is 6552.6 h, which results in a total operation downtime of 2207.4 h. A similar estimation can be drawn out for wildfire scenarios and INFERNO firefighting operational year concept for the **U**nited **S**tates of **A**merica (USA) using data from the National Centers for Environmental Information [50], [51].

Formation Flight To increase the efficiency of the fleet on longer routes and to reduce emissions, formation flight is used. Savings of up to 18 % for the following aircraft have already been demonstrated in flight tests [52], [53]. However, flight controllers available today for automated formation flight are only stable outside the wake vortex inflow area [54]. For this reason, formation flight should be carried out within the centre field. This corresponds to a distance of 15 to 150 wingspan of the aircraft. This area also has the advantage that the aircraft structure is significantly less stressed. However, the savings potential here is only up to 10 % [55], [56]. The exact sweep spot is to be found during the further development process with the help of a suitable simulation method. As a further development step, the loyal wingman concept is imaginable.

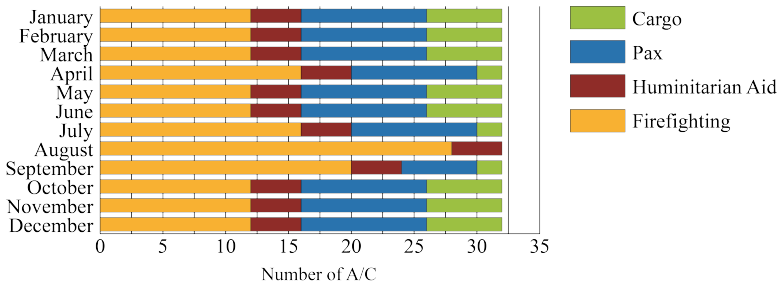

Figure 34 – Yearly fleet concept of the INFERNO aircraft

Turnaround and Ground Handling The ground handling process of the INFERNO aircraft is dominantly influenced by refueling and the water refilling process. As depicted in fig. 35, those activities can be processed simultaneous. Fig. 36 displays the calculated times for the overall turnaround at the operational base also considering the **G**round **S**upport **E**quipment (GSE) positioning and the flight preparations by the pilot. With considering a pump performance of 470 L min^{-1}, the water tank can be refilled within six min. while the refueling is calculated with five min. The critical path for the overall turnaround is the water refilling. The whole process can be realized within a 16 min time frame.

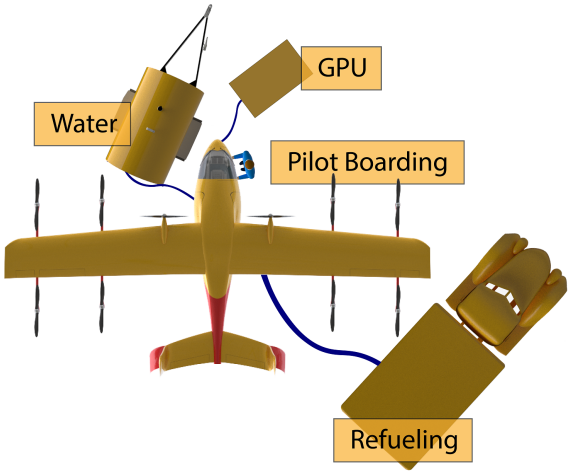

Figure 35 – Turnaround drawing

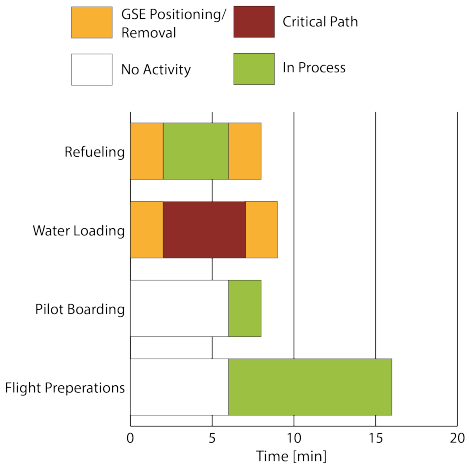

Figure 36 – Turnaround time chart

3.5 Cost Analysis

Although several unitary systems were taken into account when the parameters were calculated, all the costs pertaining to the **D**irect **O**perating **C**osts (DOC) are consistently and uniformly represented in Euros [€] throughout this section.

The Thorbeck approach, developed by J. Thorbeck of the Technical University of Berlin, is the framework used to determine the DOC for the INFERNO aircraft concept. The DOC is a direct total of the fuel costs, navigation, landing, and ground handling fees, maintenance costs, capital costs pertaining to hedge and insurance, and costs of crew.

These are the five primary costs that make up the DOC and the fig. 37 shows a graphical representation of the percentage distribution of these costs. The formulas, used for calculating the DOC from [29] adapted from the works of J. Thorbeck [57], return the cost results in 2010-€. All calculations are made with a presumed operation kick-off in 2030 and are, therefore, adjusted using the estimated rate of inflation from 2010 to 2030. By using these methods, the absolute DOC for the INFERNO program is estimated at 3.7 million €/year after taking into account the five DOC building costs. The calculated DOC per year is further broken down into 3501 €/FC, 292 €/100 km, and 58 €/100 km/Pax. The unit €/FC represents the cost per flight cycle (1200 km flight), €/100 km represents the costs per 100 flight kilometres, and €/100 km/Pax the costs per 100 flight kilometres per passenger.

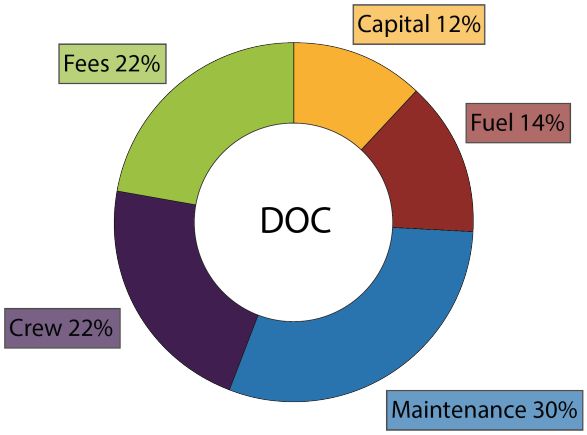

Figure 37 – Percentage distribution of the five DOC building costs

4. Conclusion

Fighting wildfires is one of the major challenges rapidly gaining significance with global warming on the rise. The INFERNO aerial firefighting concept developed as a result of the DLR Design Challenge 2022 presents a state-of-the-art aircraft designed to efficiently respond to wildfire scenarios around the globe. The concept features profound technologies to guarantee the best possible flight characteristics for these demanding missions. Thus, the INFERNO concept combines the flexibility of a VTOL aircraft with a conventional fixed-wing concept for efficiency during cruise. Thereby, both water refilling during hovering and scooping during the forward flight can be achieved leading to broad possibilities during various wildfire missions. The INFERNO aircraft is equipped with a serial hybrid system featuring a fuel efficient engine, a modern generator and a state-of-the-art battery concept supplying 10 electrically driven propeller, eight for the VTOL capabilities and two for the propulsion during forward flight. Moreover, the design is equipped with a modular fuselage part which can be flexible changed between the water tank, a passenger or a cargo module. Thus, an efficient year round fleet concept was developed minimizing ground times and operating costs. Additionally, a specific concept for the INFERNO firefighting missions was designed optimizing the amount of water carried and dropped during the operation. Therefore, a fleet of four firefighting versions is needed.

5. Contact Author Email Address

For further information about the DLR Design Challenge you can contact the organizing team:
Tobias Dietl – tobias.dietl@dlr.de; Patrick Ratei – patrick.ratei@dlr.de

For further information about INFERNO you can contact the student team:
Johannes Ritter – jo-ritter@web.de; Nicolas Mandry – mandry.nicolas@gmail.com;
Hannes Kahlo – hannes.kahlo@gmx.de; Ahmet Günay Can – guenay.ahmet.can@gmail.com;
Prishit Modi – prishitmodi7@outlook.com; Benjamin Knoblauch – Benny.knoblauch@t-online.de

6. Copyright Statement

References

[1] T. Dietl and P. Ratei, *DLR Design Challenge*. [Online]. Available: `https://www.dlr.de/content/en/articles/education/dlr-design-challenge.html` (visited on 08/29/2022).

[2] P. Shiva Prakasha, N. Naeem, P. Ratei, N. Cigal, and B. Nagel, "Exploration of aerial firefighting fleet effectiveness and cost by system of systems simulations," International Council of Aeronautical Sciences, 2021.

[3] F. Dambowsky, T. Dietl, and P. Ratei, *DLR Design Challenge 2022 – seeking ideas to fight forest fires from the air*. [Online]. Available: https://www.dlr.de/content/en/articles/news/2022/01/20220311_dlr-seeking-ideas-to-fight-forest-fires-from-the-air.html (visited on 08/29/2022).

[4] J. Hoidis, T. Dietl, and P. Ratei, *INFERNO fire-fighting aircraft takes first place in the 2022 DLR Design Challenge*. [Online]. Available: https://www.dlr.de/content/en/articles/news/2022/03/20220818_inferno-wins-dlr-design-challenge-2022.html (visited on 08/29/2022).

[5] Zki, *DLR - Earth Observation Center - MODIS Fire Service*, Jul. 2, 2022. [Online]. Available: https://www.dlr.de/eoc/en/desktopdefault.aspx/tabid-12938/22428_read-51632/ (visited on 07/02/2022).

[6] Brandon Maccherone, *Modis web*, Jul. 2, 2022. [Online]. Available: https://modis.gsfc.nasa.gov/data/dataprod/mod14.php (visited on 07/02/2022).

[7] VIKING, *Performance and Operating Data CL-415*, Viking, Ed., 2020. [Online]. Available: https://www.aerialfirefighter.vikingair.com/firefighting/performance-operating-data (visited on 06/30/2022).

[8] J. C. [Publishers], Ed., *Jane's all the world's aircraft*, Englisch, Zeitschrift, Coulsdon, Surrey, 2020.

[9] D. Finger, "Vergleichende Leistungs- und Nutzenbewertung von VTOL- und CTOL-UAVs," *Luft- und Raumfahrt*, vol. 2017, pp. 44–47, Jan. 2017.

[10] A. Bacchini and E. Cestino, "Electric VTOL Configurations Comparison," *Aerospace*, vol. 6, no. 3, 2019, ISSN: 2226-4310. DOI: 10.3390/aerospace6030026. [Online]. Available: https://www.mdpi.com/2226-4310/6/3/26.

[11] D. J. Roskam, *Airplane Design Part III: Layout of Cockpit, Fuselage, Wing and Empennage: Cutaways and Inboard Profiles*. Darcoperation, 2017, ISBN: 188488556X.

[12] D. Z. für Luft-und Raumfahrt, *100 Prozent nachhaltiger Kraftstoff zeigt Perspektive für Passagierflugzeuge*, 6.07.2022. [Online]. Available: www.dlr.de/content/de/artikel/news/2021/04/20211129_100-prozent-saf-kraftstoff-zeigt-perspektive-fuer-passagierflugzeuge.html (visited on 07/06/2022).

[13] M. Greenwood, J. M. Wrogemann, R. Schmuch, H. Jang, M. Winter, and J. Leker, "The battery component readiness level (bc-rl) framework: A technology-specific development framework," *Journal of Power Sources Advances*, vol. 14, p. 100 089, 2022, ISSN: 2666-2485. DOI: https://doi.org/10.1016/j.powera.2022.100089. [Online]. Available: https://www.sciencedirect.com/science/article/pii/S2666248522000075.

[14] Seitz, Arne and Habermann, Anaïs Luisa and Peter, Fabian and Troeltsch, Florian and Castillo Pardo, Alejandro and Della Corte, Biagio and van Sluis, Martijn and Goraj, Zdobyslaw and Kowalski, Mariusz and Zhao, Xin and Grönstedt, Tomas and Bijewitz, Julian and Wortmann, Guido, "Proof of concept study for fuselage boundary layer ingesting propulsion," *Aerospace*, vol. 8, no. 1, 2021, ISSN: 2226-4310. DOI: 10.3390/aerospace8010016. [Online]. Available: https://www.mdpi.com/2226-4310/8/1/16.

[15] M. Rendon, C. Sanchez, J. Gallo, and A. Anzai, "Aircraft hybrid-electric propulsion: Development trends, challenges and opportunities," *Sba Controle & Automacao Sociedade Brasileira de Automatica*, Jun. 2021. DOI: 10.1007/s40313-021-00740-x.

[16] D. Li, S. Zhao, A. Da Ronch, *et al.*, "A review of modelling and analysis of morphing wings," *Progress in Aerospace Sciences*, vol. 100, pp. 46–62, 2018, ISSN: 0376-0421. DOI: https://doi.org/10.1016/j.paerosci.2018.06.002. [Online]. Available: https://www.sciencedirect.com/science/article/pii/S0376042117301835.

[17] MTU AEROREPORT, *Modulare Flugzeuge: Flexibilität soll Kosten sparen*. [Online]. Available: https://aeroreport.de/de/innovation/modulare-flugzeuge-flexibilitaet-soll-kosten-sparen (visited on 07/06/2022).

[18] W. Electric, *Electric motor*. [Online]. Available: https://weflywright.com/technology#motors (visited on 07/05/2022).

[19] *LiDAR Scanners and Sensor Applications at RIEGL USA*. [Online]. Available: https://www.rieglusa.com/lidar-scanners-and-sensors-applications.html (visited on 07/11/2022).

[20] *Flightcell DZMx*, 2020. [Online]. Available: https://www.flightcell.com/products/flightcell-dzmx (visited on 07/11/2022).

[21] F. M. White and J. Majdalani, *Viscous fluid flow*. McGraw-Hill New York, 2006, vol. 3.

[22] L. Carrino, "Foreword 2," in *Morphing Wing Technologies*, A. Concilio, I. Dimino, L. Lecce, and R. Pecora, Eds., Butterworth-Heinemann, 2018, pp. li–lii, ISBN: 978-0-08-100964-2. DOI: https://doi.org/10.1016/B978-0-08-100964-2.09982-2. [Online]. Available: https://www.sciencedirect.com/science/article/pii/B9780081009642099822.

[23] D. Coutu, V. Brailovski, and P. Terriault, "Optimized design of an active extrados structure for an experimental morphing laminar wing," *Aerospace Science and Technology*, vol. 14, no. 7, pp. 451–458, 2010.

[24] B. K. Woods, J. H. Fincham, and M. I. Friswell, "Aerodynamic modelling of the fish bone active camber morphing concept," in *Proceedings of the RAeS Applied Aerodynamics Conference, Bristol, UK*, vol. 2224, 2014.

[25] M. M. S. Reza, S. A. Mahmood, and A. Iqbal, "Performance analysis and comparison of high lift airfoil for low speed unmanned aerial vehicle," International Conference on Mechanical Industrial & Energy Engineering, 2016.

[26] P. D. R. Eppler, *Airfoil Design and Data*. Springer-Verlag Berlin Heidelberg, 1990, ISBN: 978-3-662-02648-9.

[27] Prof. Dr.-Ing. Andreas Strohmayer, *Flugzeugentwurf I*.

[28] I. Buchweitz, *Flugzeugentwurf am Beispiel eines ausgeführten Flugzeugs*, Hochschule für Angewandte Wissenschaften Hamburg, Fachbereich Fahrzeugtechnik, Ed., Hamburg, Feb. 15, 2002.

[29] Prof. Dr.-Ing. Andreas Strohmayer, *Flugzeugentwurf II*.

[30] D. P. Raymer, *Aircraft design: A conceptual approach* (AIAA education series), Sixth edition. Reston, Virginia: American Institute of Aeronautics and Astronautics, Inc., 2018, ISBN: 978-1-62410-490-9.

[31] Prof. Dr. -Ing. Thorsten Lutz, *Flugzeugaerodynamik I & II*.

[32] E. Torenbeek, *Advanced Aircraft Design: Conceptual Design, Analysis and Optimization of Subsonic Civil Airplanes*. John Wiley & Sons, 2013, ISBN: 978-1-118-56811-8.

[33] PROF. DR.-ING. DIETER SCHOLZ, *Skript zur Vorlesung Flugzeugentwurf*, 1999.

[34] J. Ritter, N. Mandry, H. Kahlo, A. C. Günay, B. Knoblauch, and P. Modi, "Design of a hybrid powertrain for a next generation VTOL firefighting aircraft," will be Published at DLRK 2022, Oct. 2022.

[35] CENTRELINE, *Centreline website*. [Online]. Available: https://www.centreline.eu/innovation/ (visited on 07/10/2022).

[36] A. Seitz, F. Peter, J. Bijewitz, A. Habermann, Z. Goraj, M. Kowalski, A. Pardo, C. Hall, F. Meller, R. Merkler, O. Petit, S. Samuelsson, B Corte, M. Sluis, G. Wortmann, M. Dietz, "Concept validation study for fuselage wake-filling propulsion," Bauhaus Luftfahrt e.V., Warsaw University of Technology, University of Cambridge, Airbus Innovations, MTU Aero Enignes, Chalmers University of Technology, Technical University of Delft, Siemens AG, ARTTIC, 2018.

[37] S. Metals, *Inconel alloy 625*. [Online]. Available: https://www.specialmetals.com/documents/technical-bulletins/inconel/inconel-alloy-625.pdf (visited on 07/11/2022).

[38] S. Gudmundsson, *General aviation aircraft design: Applied methods and procedures*, 1st ed. Oxford, UK: Butterworth-Heinemann, 2014, ISBN: 978-0-12-397308-5.

[39] W. Lijing, X. Wei, H. Xueli, *et al.*, "The virtual evaluation of the ergonomics layout in aircraft cockpit," in *2009 IEEE 10th International Conference on Computer-Aided Industrial Design & Conceptual Design*, IEEE, 2009, pp. 1438–1442.

[40] Yeh, Michelle and Swider, Cathy and Jo, Young Jin and Donovan, Colleen and others, "Human Factors Considerations in the Design and Evaluation of Flight Deck Displays and Controls," John A. Volpe National Transportation Systems Center (US), Tech. Rep., version 2.0, 2016.

[41] *Talon MMS*. [Online]. Available: https://www.flir.com/products/talon-mms/ (visited on 07/11/2022).

[42] AgAir Update Staff, *Caci's aerial sensor technology provides real-time heat mapping data and reduces risk to firefighters*, Oct. 2020. [Online]. Available: https://aerialfiremag.com/2020/10/27/cacis-aerial-sensor-technology-provides-real-time-heat-mapping-data-and-reduces-risk-to-firefighters (visited on 07/11/2022).

[43] G. Penney, D. Habibi, M. Cattani, and M. Carter, "Calculation of critical water flow rates for wildfire suppression," *Fire*, vol. 2, no. 1, 2019, ISSN: 2571-6255. DOI: 10.3390/fire2010003. [Online]. Available: https://www.mdpi.com/2571-6255/2/1/3.

[44] R. Hansen, "Corrigendum to: Estimating the amount of water required to extinguish wildfires under different conditions and in various fuel types," *Wildland Fire*, vol. 21, p. 778, 2012. DOI: 10.1071/WF11022_CO.

[45] K. Satoh, I. Maeda, K. Kuwahara, and K Yang, "A numerical study of water dump in aerial fire fighting," *Fire Safety Science*, vol. 8, pp. 777–787, 2005.

[46] European Union Aviation Safety Agency, *Certification Specifications and Acceptable Means of Compliance for Normal, Utility, Aerobatic and Commuter Aeroplanes CS-23: CS-23*, 2020.

[47] I. Geiß and A. Strohmayer, *Operational Energy and Power Reserves for Hybrid-Electric and Electric Aircraft*. Deutsche Gesellschaft für Luft- und Raumfahrt - Lilienthal-Oberth e.V., 2021.

[48] D. Aifantopoulou *et al.*, "Copernicus emergency management service," *10442/15383*, pp. 01–54, 2016.

[49] *Welcome to EFFIS*. [Online]. Available: https://effis.jrc.ec.europa.eu/.

[50] National Centers for Environmental Information (NCEI), *Wildfires Report | National Centers for Environmental Information (NCEI)*. [Online]. Available: https://www.ncei.noaa.gov/access/monitoring/monthly-report/fire/202112 (visited on 07/11/2022).

[51] United States Environmental Protection Agency (EPA), *Climate Change Indicators: Wildfires*. [Online]. Available: https://www.epa.gov/climate-indicators/climate-change-indicators-wildfires (visited on 07/11/2022).

[52] M. Vachon, R. Ray, K. Walsh, and K. Ennix, "F/a-18 performance benefits measured during the autonomous formation flight project," Oct. 2003. DOI: 10.2514/6.2002-4491.

[53] C. Hanson, J. Ryan, M. Allen, and S. Jacobson, "An overview of flight test results for a formation flight autopilot," in *AIAA Guidance, Navigation and Control Conference and Exhibit*, [Reston, Va.]: [American Institute of Aeronautics and Astronautics], 2002, ISBN: 978-1-62410-108-3. DOI: 10.2514/6.2002-4755.

[54] A. K. R. Luckner, "Formationsflug von Verkehrsflugzeugen zur Treibstoffeinsparung," [Online]. Available: https://www.dglr.de/publikationen/2016/370376.pdf (visited on 07/01/2022).

[55] S. R. Bieniawski, S. Rosenzweig, and W. B. Blake, "Summary of flight testing and results for the formation flight for aerodynamic benefit program," in *52nd Aerospace Sciences Meeting*, ser. AIAA SciTech Forum, Reston, Virginia: American Institute of Aeronautics and Astronautics, 2014, ISBN: 978-1-62410-256-1. DOI: 10.2514/6.2014-1457.

[56] T. C. Flanzer and S. R. Bieniawski, "Operational analysis for the formation flight for aerodynamic benefit program," in *52nd Aerospace Sciences Meeting*, Reston, Virginia: American Institute of Aeronautics and Astronautics, 2014. DOI: 10.2514/6.2014-1460.

[57] J Thorbeck, "Manuskript zur integrierten Lehrveranstaltung Flugzeugentwurf I und II," TU Berlin, Oct. 2003.